InterPore JOURNAL

Original Research

INHERENT ERRORS IN CURRENT CORE-FLOODING RELATIVE PERMEABILITY DATA FOR MODELLING UNDERGROUND HYDROGEN STORAGE

Gang Wang, Alan Beteta, Kenneth S. Sorbie, Eric J. Mackay

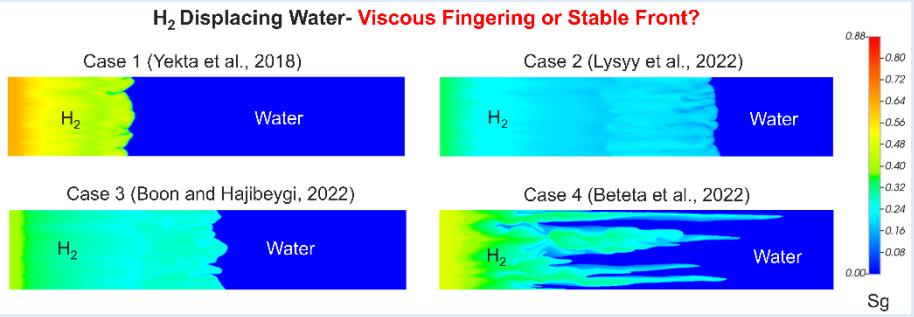
Heriot-Watt University, Edinburgh, United Kingdom

Correspondence to:
Gang Wang,
g.wang@hw.ac.uk

How to Cite:
Wang, G., Beteta, A., Sorbie, K. S., & Mackay, E. J. (2025). Inherent Errors in Current Core-Flooding Relative Permeability Data for Modelling Underground Hydrogen Storage. *InterPore Journal*, 2(1), IPJ260225–6.
https://doi.org/10.69631/ipj.v2i1nr42

RECEIVED: 16 Sept. 2024
ACCEPTED: 20 Jan. 2025
PUBLISHED: 26 Feb. 2025

ABSTRACT



In the design and optimization of an underground hydrogen (H_2) storage facility in an aquifer or other reservoir system, the H_2/water relative permeabilities (RP) are the most critical two-phase data for input to numerical simulation. In this paper, we present a critical analysis of the published experimental H_2/water RP functions in the literature. We present fine-grid simulations of H_2 displacing water (denoted H_2 → water) using three of the most widely cited steady-state RP datasets (13, 20, 38) in a mildly heterogeneous permeability field, at a field length scale of ~100m. Since the viscosity ratio between water and H_2 is (μ_w/μ_{H2}) ≈ 70, then at some length scale above a few meters, it is *inevitable* that the system must show immiscible viscous fingering of the H_2 into the water phase. Indeed, the emergence of viscous fingering at some length scale is a "sense check" that the input data used in the simulations are correct, especially the H_2/water relative permeability functions.

In fact, none of the three published H_2/water RP curves leads to viscous fingering. Instead, they all show stabilized flood fronts. The reasons for this are due to shortcomings of the (conventional) gas/liquid experimental methods used to obtain the RP functions. These methods yield RP functions at the wrong force balance between the capillary, gravity and viscous forces. For fingering to emerge, it is necessary to derive the viscous dominated RP functions. An alternative, more physically appropriate set of viscous dominated "fingering RP functions" is proposed and applied. When applied

at the core scale, these new RP functions show fully dispersed flow, as they do when applied in a vertical (downwards) gravity stable displacement. However, the viscous fingering emerges naturally in horizontal flow as the length scale of the system increases and viscous forces become dominant.

KEYWORDS
Hydrogen storage, Computational flow dynamics, Viscous fingering, H_2/water relative permeability

@2025 The Authors

This is an open access article published by InterPore under the terms of the Creative Commons Attribution-NonCommercial-NoDerivatives 4.0 International License (CC BY-NC-ND 4.0) (https://creativecommons.org/licenses/by-nc-nd/4.0/).

1. INTRODUCTION AND BACKGROUND

1.1. Background to Underground Hydrogen Storage (UHS)

As a clean-burning energy vector, hydrogen (H_2) is expected to play a crucial role in the future energy mix. Its ability to store renewable energy and address intermittency issues, potentially makes it a key player in pursuing energy security and sustainability goals (1). However, the volumetric energy density of H_2 is much lower than that of gasoline (2). This means the amount of H_2 required to achieve the Net-Zero goal will be enormous (33). For small to medium-scale H_2 storage (megawatt level), line packing and salt caverns are considered to be viable solutions, and these are currently being actively developed (4). However, for the seasonal energy storage at the gigawatt scale necessary to support widespread adoption of H_2 energy, these methods alone are not adequate. Subsurface porous media, such as saline aquifers and depleted hydrocarbon reservoirs, are feasible options for large-scale H_2 storage (40). These geological formations provide significant storage capacity while also offering an economic advantage by repurposing existing infrastructure, thereby reducing overall costs.

1.2. Numerical Assessment of UHS and H_2/Water Relative Permeability

To determine the viability of UHS in porous media, it is important to assess key influencing factors and potential risks for field applications. A primary challenge lies in understanding the complex multiphase flow behavior during UHS operations (5). This understanding is essential for optimizing storage performance, particularly in terms of net recovery and H_2 purity during back production (34, 36). As with other subsurface applications, computational fluid flow modelling in porous media is a powerful tool for analyzing reservoir behavior in UHS projects. The rigor and reliability of these simulations are greatly influenced by various input parameters, such as the geological characteristics, the permeability structure of the porous formation, fluid properties, etc. Of the multi-phase flow parameters, relative permeability is the most important since it plays a central role in governing the two-phase flow dynamics in UHS operations. The gas/liquid relative permeability (RP) functions are primarily related to the *viscous* forces in the system, although in the two-phase flow equations, they are coupled with both gravity and capillary forces, and while various formulations of these equations exist, they are all equivalent (3, 22, 24, 37). Capillary pressure (P_c) plays a local role (at shorter length scales) acting like a non-linear dispersivity term in a frontal displacement (7, 16, 39); capillary dispersivity can be dominant at the small (core) scale but, since it is a highly local effect, it reduces in influence as the system size increases and viscous and gravity forces become more prominent.

For a gas-liquid system, the relative permeabilities of each phase can be determined through either steady-state (SS) or unsteady-state (USS) core flooding experiments (15). Both SS and USS RP determination involve measuring fluid saturations, pressure differences, and flow rates, from which relative permeability is calculated. The SS method involves simultaneous injection of both liquid and gas phases and assumes a uniform saturation profile throughout the (one-dimensional; 1D) core sample. The USS method involves the displacement of one phase by another (both gas → water and water → gas) and the multidimensional core flooding problem is usually reduced to a 1D problem for mathematical analysis to find the RP functions (16). In general, gas has a much lower viscosity than the

water phase and thus viscous fingering (non-uniform frontal saturation profiles) would normally occur during USS horizontal displacements. To "mitigate" this effect, USS core flood tests are sometimes conducted on vertically oriented samples for gas-water systems (19, 21). This orientation invokes gravity to "stabilize" the gas-liquid interface, resulting in a more uniform displacement front (26, 30). Indeed, even SS gas/liquid floods are often conducted in a vertical (downwards) orientation to avoid gravity segregation (14). While the displacing front is successfully stabilized, gravity may significantly alter the derived relative permeability, shifting it from a viscous-dominated regime to a viscous/gravity influenced system. Additionally, capillary pressure also causes significant inter-phase mixing in typical core-scale systems, a phenomenon known as capillary dispersion, which may further stabilize the flowing front (27). Thus, RP experiments, both SS and USS, may be carried out at an uncertain combination of viscous, capillary and gravity forces, and this can be very important in determining the "correct" RP functions in a gas/liquid system.

The methods for determining both SS and USS RP functions described briefly above have been extensively applied in studies on CO_2 sequestration and hydrocarbon recovery (6, 21). Recently, the UHS research community applied these methods to derive H_2-water relative permeability functions (13, 20, 38). However, to date we are not aware of any flow simulation study to "sense check" these H_2/water published RP functions, in the terms described in the following subsection.

1.3. Viscous Instability and "Sense Check" on Current H_2/water RP Results

In an UHS project, H_2 gas will displace water when it is injected into an aquifer during H_2 storage. In this immiscible displacement, the water/gas viscosity ratio $\left(\mu_w/\mu_g\right)$ is approximately 70. It is therefore certain that, *at some length scale*, immiscible viscous fingering (VF) will occur, thus leading to an inefficient frontal displacement region and much more fluid mixing than occurs in a piston-like stable displacement. The damping forces on immiscible viscous fingering at the smaller (i.e. core) scale are capillary dispersion and, to a lesser extent, local hydrodynamic dispersion due to the heterogeneity of the porous medium. It has been shown by Beteta et al (10) using scaling theory that, when the correct viscous dominated relative permeabilities are used then, at the small scale no fingers are observed due to capillary dispersion (when $P_c \neq 0$). However, as the system size increases, viscous forces increase and capillary forces remain the same, and therefore at some length scale, the viscous forces dominate, and the viscous fingering will emerge. Therefore, if one is given an "experimental" core-scale RP for the H_2/water system, it is a ***requirement*** that as the system size increases, even in a "slightly heterogeneous" permeability field, that viscous fingering is observed at some point (i.e. at some length scale). What this length scale is depends on the magnitude of the capillary dispersivity, but typically it will be in the approximate range of ~1 – 20m; obviously, a length which is *much* larger than the core scale, but much smaller than the full field scale. This emergence of viscous fingering at some length scale is the "sense check" on RP functions which we referred to above.

In this work, we have systematically examined a range of published SS RP functions in 1D and two-dimensional (2D) flow simulations of H_2 displacing water (denoted H_2 → water), and the results are reported below for three of them (13, 20, 38). All three RP functions are based on steady-state methods using real rock samples. Yekta et al. (38) used samples from Adamswiller quarry, while Lysyy et al. (20) and Boon and Hajibeygi (13) used Berea rock. Both Yekta et al. (38) and Lysyy et al. (20) utilized vertical cores with fluid injection from the top and production from the bottom. In contrast, the experimental work by Boon and Hajibeygi (13) was conducted using a horizontal core setup. If one conducts a fine grid 2D (or 3D) H_2 → water displacement simulation in a simple heterogeneous permeability field (a correlated random field, CRF, in this work) using *any* of these published RP functions, they all predict *stable* displacement and show no evidence of viscous fingering. Thus, they fail our "sense check". We regard this as due to an "inherent error" in the way in which the relative permeabilities have been measured. However, we note that this is *not* a criticism of the experimental groups who have produced these experimental results. All of these literature H_2/water RP papers use very conventional experimental methods for measuring steady-state gas/water relative permeability curves, but we believe that these methods are deeply flawed.

In previous work, we have presented what we believe are more physically correct methods for obtaining RP functions in two phase immiscible fingering systems (10, 31). These new simulation methods have been applied to analyze the results from core floods in which we assume the presence of viscous fingering, and 2D slab flood experiments where viscous fingering is directly observed via x-ray scanning (8). These methods have also been applied very successfully to the modelling of other viscous fingering experiments in the literature (10, 28). In brief, the problem is that very small (core) scale gas water experiments are "measuring" the "wrong" RP since the system is too capillary dispersed locally (or stabilized too much by gravity), and the local total mobility (λ_T) of the two phase system is too low. Recall that mobility of a phase is $\lambda_w = \left(k_{rw}/\mu_w\right)$ and $\lambda_g = \left(k_{rg}/\mu_g\right)$ for water and gas, respectively, and the total mobility is $\lambda_T = \left(\lambda_w + \lambda_g\right)$. These observations are shown experimentally by Beteta et al (11). We use these methods to derive a more physically realistic RP function for the H_2/water system, with $\left(\mu_w/\mu_g\right) \approx 70$, which exhibits viscous fingering at the larger scale while showing fully dispersed flow at the core scale. We have also used scaling theory to show how this leads to emergent immiscible fingers at the larger scale in the H_2/water system.

It may be thought that a pore scale modelling approach would be useful to address the problem of the inadequacy of the H_2/water RP functions. However, while pore-scale modelling offers valuable insights into fundamental flow dynamics, it has significant limitations for deriving field-scale relative permeability functions. The primary constraints are twofold: pore-scale models predominantly capture localized phenomena, and their results are dominated by capillary effects alone. Indeed, our analysis suggests that going down to the pore scale is looking in the "wrong direction" and our results suggest we need to look at the *global* state of the system. Therefore, this study deliberately concentrates on core-flooding experimental methodologies and the scale up of these to the field using scaling theory (10, 24, 35).

In summary, we point out the misconceptions in selecting flow functions for modelling the multiphase UHS system. We systematically reviewed and evaluated a range of H_2/water relative permeabilities from literature using our 2D fine-scale simulations. In particular, three widely cited SS RP datasets (13, 20, 38) for H_2 and water were examined to demonstrate how the inherent errors in conventional RP measurement methods can lead to misleading predictions of the flow behavior. We present an example of "fingering" RP functions which are more qualitatively correct in their predicted flow behavior. The scale dependence of the capillary pressure and the emergence of viscous fingering with length scale are also discussed and illustrated by numerical examples.

2. NUMERICAL SIMULATION METHODOLOGY

2.1. The Numerical Simulation Model

Figure 1 shows the correlated 2D horizontal permeability field used in the calculation presented here. This correlated random field (CRF) was generated using the Petrel software to mimic the minor heterogeneity in a simple aquifer reservoir model (29). The model dimensions are 100 m by 20 m, with a fine grid resolution of 0.1m in all directions to accurately capture any fingering patterns in the saturation distribution which may occur over time, i.e. $S_w(x, y, t)$ or $S_g(x, y, t)$. The permeability follows a

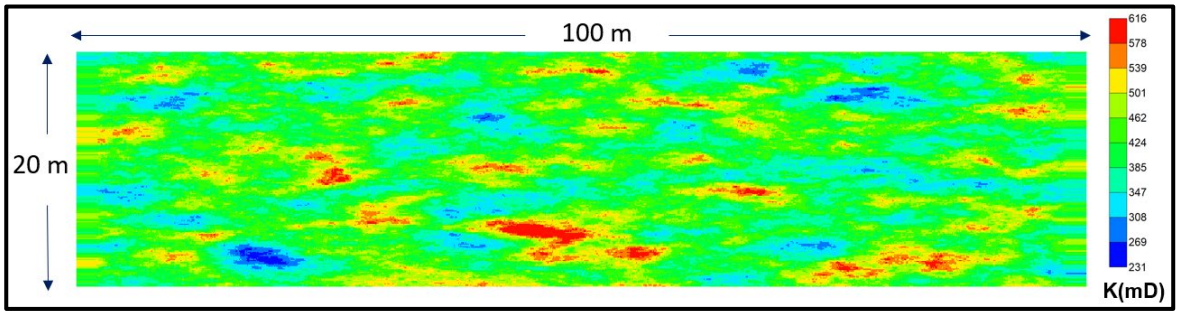


Figure 1: The heterogeneous permeability field configured to induce flow of interest; this field represents a porous medium with a relatively low permeability contrast.

log-normal distribution, ranging from approximately 200 mD to 600 mD across the formation. The permeability heterogeneity is characterized by a Dykstra-Parsons coefficient of 0.13, indicating a relatively low degree of permeability variation. The porosity is set to a constant value of 0.1. The correlation range is 10 m in the x-direction and 2 m in the y-direction, respectively.

All flow simulations are conducted using a full-compositional simulator CMG/GEM based on the Equation of State (EOS) fluid model of Peng and Robinson (23). The input values are drawn from our previous work, which has validated the key fluid properties (35). This will allow us to build future studies involving multi-component systems based on this work. One horizontal injection well and one horizontal production well are positioned at either end of the model (at x = 0 and x = 100m). The injector is perforated across the entirety of the left side, while the producer is perforated along the entire right side. The injection rate is set at 0.05 pore volumes per day (PV/day) and saturation patterns are shown after 3 days (0.15PV) of injection. The producer is operated with a bottom-hole pressure (BHP) constraint equal to the initial reservoir pressure of 130 bar to mimic a constant pressure boundary. No gas breakthrough to the producer occurs in any of our simulations presented in this work.

2.2. The Flow Functions – Relative Permeabilities and Capillary Pressure

As previously discussed, many studies have utilized standard core flooding techniques to determine the relative permeability of H_2 and water. Our research evaluates three widely cited datasets to highlight the limitations of this method in the context of UHS (13, 20, 38). The reported RP functions are plotted collectively in **Figure 2.** Note that Case 3 uses RP functions directly from Bo et al (12), who applied the Brooks-Corey-variable Corey model to extend original data from Boon and Hajibeygi (13). Capillary pressure is excluded to maximize the potential for viscous instability in our 2D areal "sense-checking" simulations.

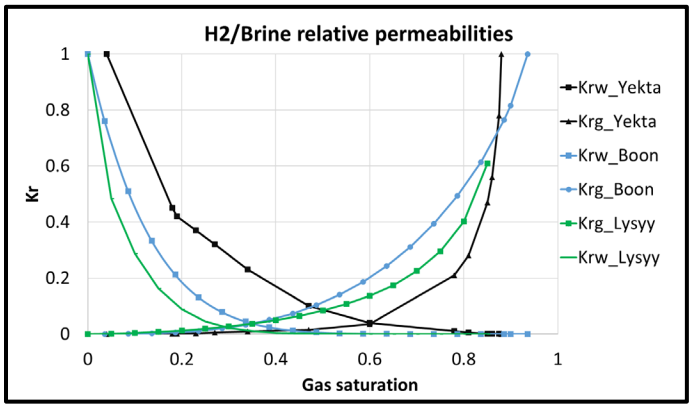


Figure 2: Relative permeability curves for H_2-water systems from three publications in the literature.

Both 1D and 2D flow simulations were conducted to illustrate the flow patterns predicted by these various RP functions. For comparison, a "fingering" RP model adapted from a water-oil system is incorporated to illustrate the presence of viscous instability in the configured system (9). This is denoted as Case 4 and is shown in **Figure 3** (left side). This dataset was selected because it has been experimentally and numerically validated for modelling immiscible viscous fingering phenomena. Refer to **Figure 1S** in the **Appendix** (available online) for their CT scan results showing the fluid distribution during the core-flooding displacement. The unusual form of the Case 4 RP has been noted in our previous publications, but it provides an excellent match to experimental data, and can be explained straightforwardly (10, 28, 31). See in particular the discussion in the Appendix to Salmo et al (28). In this earlier work, the water displacing oil injection was a drainage process (non-wetting phase displacing a wetting phase), which is the case in the water displacements by H_2. Therefore, in our adaptation, the water relative permeability (k_{rw}) from Beteta et al (9) was used as the gas relative permeability (k_{rg}) in this work, and similarly, their oil relative permeability (k_{ro}) for our liquid relative permeability (k_{rl}).

The central difference between conventional RP derivation methods and that used here to obtain the RP function in **Figure 3** for systems that are viscous unstable lies in the *assumed model of the flow*. The objective of all methods is to match pressure drop, fluid saturations (if available), and gas/water recovery data. The conventional assumed model is usually a 1D system, and often Corey curves are taken as the RP functions. Data is often matched through history matching of the core flood (usually in 1D) using

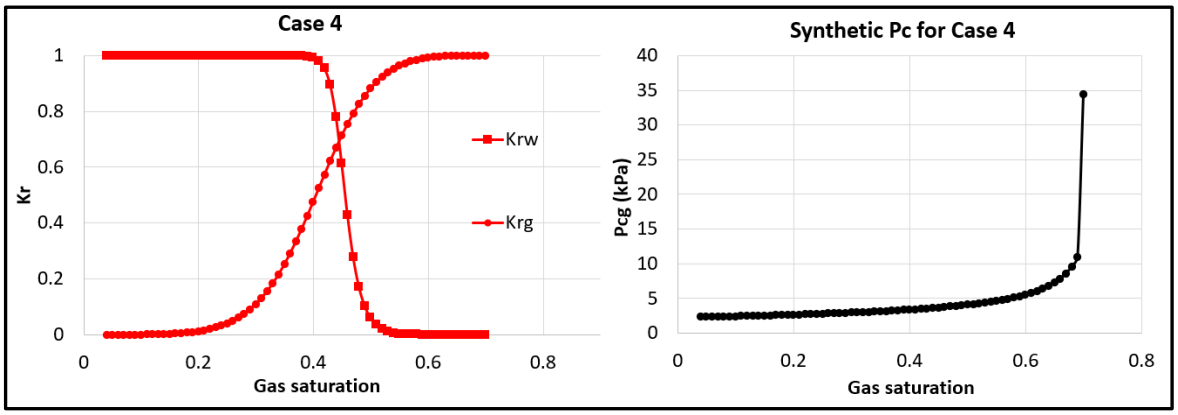


Figure 3: Relative permeability published by Beteta et al. (9) and synthetic capillary pressure.

numerical simulation and parameter adjustments to achieve the best fit. This method is "blind" to any fingering phenomena that take place (it is 1D). Our method assumes that fingering will take place, and it models the system as a 2D (or 3D) model. It then aims to match the system's fractional flow, pressure drop, and fluid saturations, incorporating LET correlations to establish initial relative permeability curves. The final relative permeability is then selected from multiple candidate curves by maximizing the total mobility, as explained in detail in previous papers (9, 31).

To illustrate the scale-dependent dispersion effect of capillary pressure, a synthetic capillary pressure curve (right side of **Fig. 3**) with a typical gas-liquid maximum value of 35 kPa (~5psi) is incorporated in our simulations. This synthetic capillary pressure is applied only in Case 4 in which the RP function is based on the data of Beteta et al (9), as it is the only scenario exhibiting viscous fingering. In Case 4, the model size is adjusted by modifying the grid cell dimensions (Δx and Δy), while maintaining a constant pore volume injection rate of 0.05 PV/day under reservoir conditions to achieve different balances between viscous and capillary forces. This approach demonstrates how capillary pressure can mitigate and mask viscous instabilities at small scales but not at larger scales. It is shown in Section 3.2, the cases derived from three sets of actual H_2/water relative permeabilities from literature do not display viscous fingering, regardless of capillary pressure.

2.3. Description of the Simulations Presented

Both 1D and 2D fine grid simulations have been carried out in this work to illustrate the points discussed in the previous sections, and to explain how we reached our conclusions. The work structure and the rationale of each of the simulation tests are outlined in **Table 1**.

Table 1: Simulation scenarios and objectives.

Step	Scenarios			Objectives
# 1	1D simulation based on all four sets of relative permeabilities.			To compare the gas saturation profiles and gas saturation front height at the displacing front for each of the 4 cases.
# 2	Case 1 (38)	Vs.	Case 4 (9)	To "sense check" the existing RP functions without Pc by testing the emergence of viscous fingering in 2D areal simulations.
	Case 2 (20)			
	Case 3 (13)			
# 3	2D vertical simulation of Case 4			To demonstrate the stabilizing effects of gravity on RP functions in a 2D vertical simulation.
# 4	Reduced size of Case 4 (100 times smaller)	Vs.	Corresponding cases with synthetic P_c	To illustrate the scale-dependent impact of capillary pressure on flow behavior.
	Reduced size of Case 4 (4 times smaller)			
	Original Case 4			
	Enlarged size of Case 4 (25 times larger)			

3. RESULTS AND DISCUSSION

3.1. The 1D Simulations and Fractional Flow Functions

The first (#1) stage of the study (**Table 1**) involved carrying out a series of one-dimensional (1D) simulations using reported literature RP data. A homogeneous model with permeability k = 500 mD at 100% saturation water (S_w = 1) was used. Despite the assumption of incompressible fluid in the construction of the fractional flow profiles, a good estimate of the shock front gas saturations (S_{gf}) at the displacing front is obtained. As seen in **Figure 4**, the gas saturation at the displacing front is lowest in the case with data by Lysyy et al (20) whereas highest in the case with data by Yekta et al (38). Based on these one-dimensional experimental and numerical results, a preliminary assessment suggests that the flow in the subsequent 2D simulations is likely most unstable in the Case 2 (20) and most stable in the Case 1 (38). The Case 4 1D saturation profile (modified from Beteta et al (9)) in **Figure 4** lies in the middle of the "experimental" RP cases, at the apparently "stable" end of this set close to that of Yekta (38). Our forthcoming 2D simulations using these H_2-water relative permeabilities will show the predicted flooding patterns arising from these RP functions.

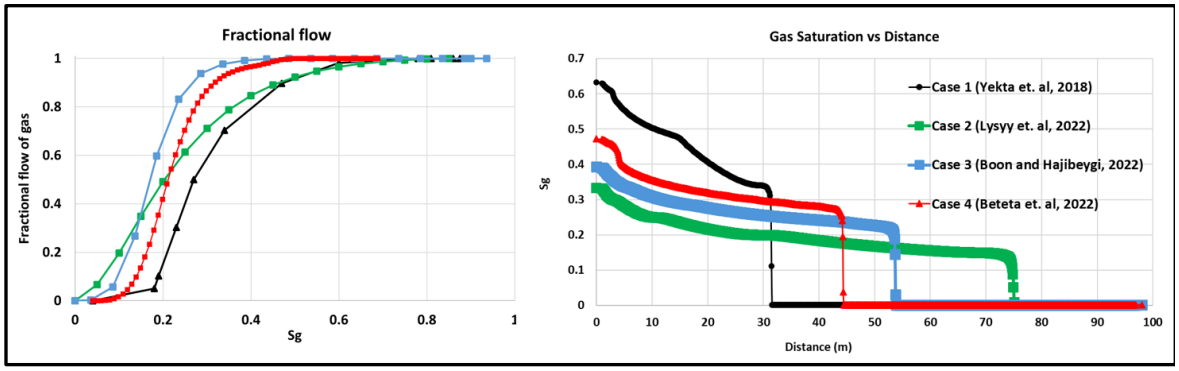


Figure 4: Fractional flow functions arising from the experimental RP curves of Cases 1 – 4 (**Table 1**) and their corresponding gas displacement fronts in1D simulations (S_g front height, S_{gf}) after 0.15PV of H_2 injection.

3.2. 2D Areal Simulations of Water Displacement by Hydrogen (Sense check)

In Step 2 of this study (**Table 1**), 2D simulations of H_2 injection into water-saturated zones were conducted. These simulations used all four sets of relative permeability data without capillary pressure (Cases 1 – 3 for the published RP cures and Case 4 as described previously). In these initial simulations, there was no capillary pressure (P_c = 0), and thus only viscous forces were acting. Hence, the only dispersive force in the simulation was the numerical dispersion, which was very small due to the very fine grid being used. According to Jessen et al (17), the dispersivity (α) from the grid is $\alpha \sim \Delta x/2 \sim 0.05\text{m}$ for the numerical scheme used, which leads to a grid Peclet number of $N_{Pe,grid} \sim 2Nx$ = 2000. This is clearly advection (viscous) dominated, as can be seen from the simulated shock front structure in **Figure 4**.

The predicted 2D saturation profiles of all four RP cases after 0.15 PV of H_2 injection are plotted in **Figure 5**. Given that the viscosity ratio between hydrogen (0.008 mPa·s) and water (0.53 mPa·s) is approximately $(\mu_w/\mu_g) \sim 70$, severe gas fingering should theoretically occur. Surprisingly, none of the three published H_2-water relative permeability datasets produced the expected viscous fingering flow of hydrogen. In contrast, very evident viscous fingering occurred in Case 4, which is based on the relative permeability data from Beteta et al (9). In other words, all three RP functions in literature failed in our "sense check" analysis.

 https://doi.org/10.69631/ipj.v2i1nr42

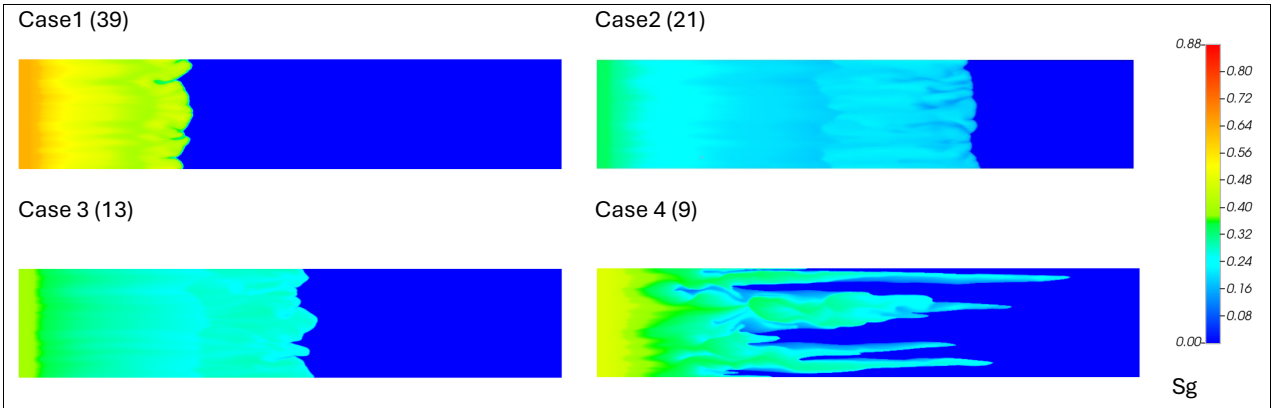


Figure 5: Gas saturation profile after 0.15 PV H_2 injection in the four cases.

To understand why viscous fingering is entirely smeared out in Cases 1-3 where the published experimental SS RPs were used, we review (i) the precise forms of these relative permeability curves, and (ii) the experimental procedures described in the three papers. As seen in **Figure 2**, all these experimental results indicate very low gas mobility, even at gas saturations up to 0.5 (k_{rg} ~ 0.1) during the initial drainage process. **Figure 6** shows a comparison of the total mobility, λ_T vs. S_g; recall that $\lambda_T(S_g) = (\lambda_w + \lambda_g) = (k_{rw}/\mu_w) + (k_{rg}/\mu_g)$. Note that all of the experimental cases (1 to 3) show much lower λ_T functions than the Case 4 "fingering" RP case. Obviously, these functions are suppressed by the low gas mobility at high S_g, and this low mobility causes a pressure build up in the finger, which in turn suppresses finger formation. The RP of Case 4 was actually constructed deliberately as "maximum mobility" RP functions (31) in order to correctly reproduce immiscible viscous fingering (9).

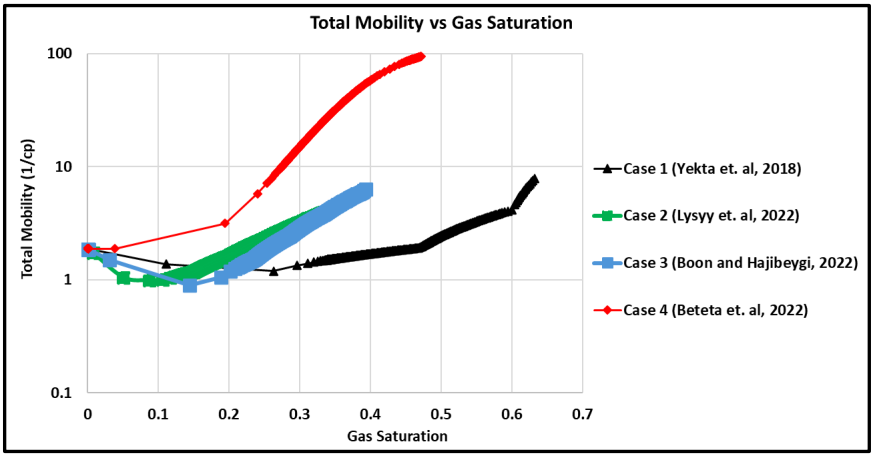


Figure 6: Total mobility varying with gas saturations of four cases (1D simulations).

We may ask: *Why do the experimental SS RPs give such low mobilities*? The answer to this question is partly theoretical and partly practical, as we explain below. From a theoretical perspective, we noted that the relative permeability is related to ***viscous*** forces. To be unique, we would like to measure this quantity under *viscous dominated* conditions, i.e. free from the influence of the other two forces of gravity ($\Delta\rho g$) and capillarity. As mentioned earlier, the flooding experiments (Case 1 & 2) conducted by Yekta et al (38) and Lysyy et al. (20) were based on a vertical set-up to better achieve the steady-state two-phase flows by avoiding gravity override (preferential gas flow at the top). However, the displacement will then be affected by gravity forces as well as by both capillary and viscous forces. In this case, the stabilization from gravity will affect the RP functions, again leading to an RP which is correct for describing a similar gravity stable displacement, but not appropriate when viscous forces alone dominate; such a RP function will be "over stable" in a 2D adverse viscosity displacement in the absence of gravity (i.e. in a horizontal direction). In addition, from a practical perspective, the gas/liquid RP

experiments are typically performed using small cores. Therefore, capillary forces will almost certainly play an important role in the core flooding experiments. For this reason, although the flooding experiments (Case 3) by Boon and Hajibeygi (13) were conducted in a horizontal direction, capillary dispersion has overly stabilized the viscous fingering patterns. Such flow experiments are therefore not suitable for capturing flow behavior at the field scale, where viscous flow regimes typically occur.

In summary, locally in a small core, the effects of both capillarity and gravity tend to lead to very disperse gas/liquid distributions which will have a lower mobility $\left(\lambda_t(S_g)\right)$, rather than more realistic fingering, which overall will have much higher total mobility. These effects are clearly demonstrated in recent work by this author group, modelling H_2 → water displacements in larger 2D sandstone slabs monitored by X-ray scanning (8), as well as in analogue water → oil or air → water experiments using a very similar viscosity ratio.

3.3. Stabilization Effects by Gravity Force on RP functions

Simulations varying the balance between viscous, gravity and capillary forces are conducted to validate our hypothesis mentioned in the last section. Case 4, which does exhibit viscous fingering, was used to simulate the system in a vertical (downward flowing) orientation to allow gravitational forces to take effect. All other parameters for this vertical case remain the same as in the original horizontal Case 4 setup. This is the third step of the simulations.

The results are shown in **Figure 7** where, as expected, the viscous fingering is eliminated. However, as shown previously (**Fig. 5**; Case 4), using the viscous dominated Case 4 RP functions in the simulations allows fingering to emerge when the system orientation is horizontal. To minimize the stabilizing effect of gravitational force on RP functions, we recommend that H_2-water relative permeability tests be conducted in a horizontal orientation. At a high enough flow rate, this approach reduces the influence of gravitational forces on the displacing front, ensuring that viscous forces remain dominant rather than being suppressed. In other words, the fingering flow pattern should be sustained and reflected in core flooding experiments.

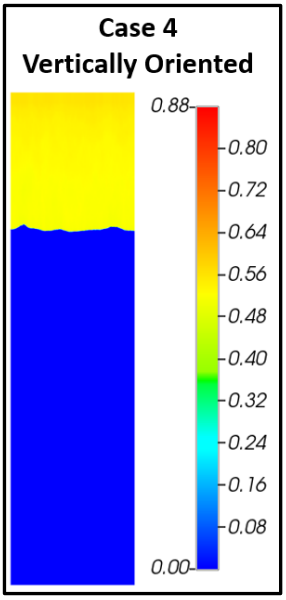


Figure 7: Gas saturation after 0.15 PV of H_2 injection in vertically orientated simulation of Case 4.

Conventional calculation methods tend to simplify core floods as 1D linear displacements based on Buckley-Leverett theory. Beteta et al (9) propose matching experimental results with a 2D (or 3D) simulation approach, assuming the presence of viscous fingers (when they are known to occur), and using a numerical scheme designed to match such experiments (31). This approach better captures the viscous-dominated immiscible fingering flow patterns occurring in gas-water systems.

In some experimental scale cases, both gravity and viscous forces may be significant. But in this work, we have only addressed the influence of gravity forces by demonstrating that when using a "fingering RP function" in gravity stable conditions, a non-fingering H_2 → water displacement results (see **Fig. 7**). This is as expected, however if RP functions are derived from the core-scale measurements of such a flood (i.e. ΔP and fluid recoveries of water and gas vs. PV), then this does not result in a "fingering RP function", due to the over-stable conditions. Therefore, this "experimentally derived" RP function will be incorrect for purely viscous dominated flow, although it may be adequate for modelling gravity stable downward displacement. Regardless of the importance of gravity, if the RP function does not lead to fingering under viscous dominated conditions, it is incorrect for simulating field scale flows where $\left(\mu_w/\mu_g\right) >> 1$. In this paper, we do not address how to separate viscous fingering and gravity effects, other than by making gravity negligible—such as by conducting viscous-dominated experiments in thin 2D slabs or performing very high-rate, long core horizontal

 https://doi.org/10.69631/ipj.v2i1nr42

floods. Therefore, we cannot provide a clear conclusion for the "mixed" case. However, work is currently in progress to resolve this matter.

3.4. Scale-dependent Capillary Dispersivity

As discussed, the effect of capillary pressure (capillary dispersivity) is very significant at the core scale. As with gravity, the capillary dispersivity will affect the experimental measurement of the "true" viscous-dominated relative permeability. The focus of this section (Step #4 in **Table 1**) is on the scale-dependent influence of capillary pressure. To analyze this, the model size is varied by adjusting the cell dimensions while maintaining the same pore volume injection rate (0.05 PV/day) under reservoir conditions. This creates the following four scenarios: one with cell size reduced by 10 times in both x and y directions, one with halved cell size, one with the original size (Case 4), and one with cell size increased by 5 times in horizontal directions, as noted in **Table 1**. The synthetic capillary pressure shown in **Figure 3** is then included in each model for comparison. **Figure 8** shows gas saturation profiles after 0.15 PV injection for all six cases, with the left column showing scenarios without capillary pressure ($P_c = 0$) and the right column including it ($P_c \neq 0$).

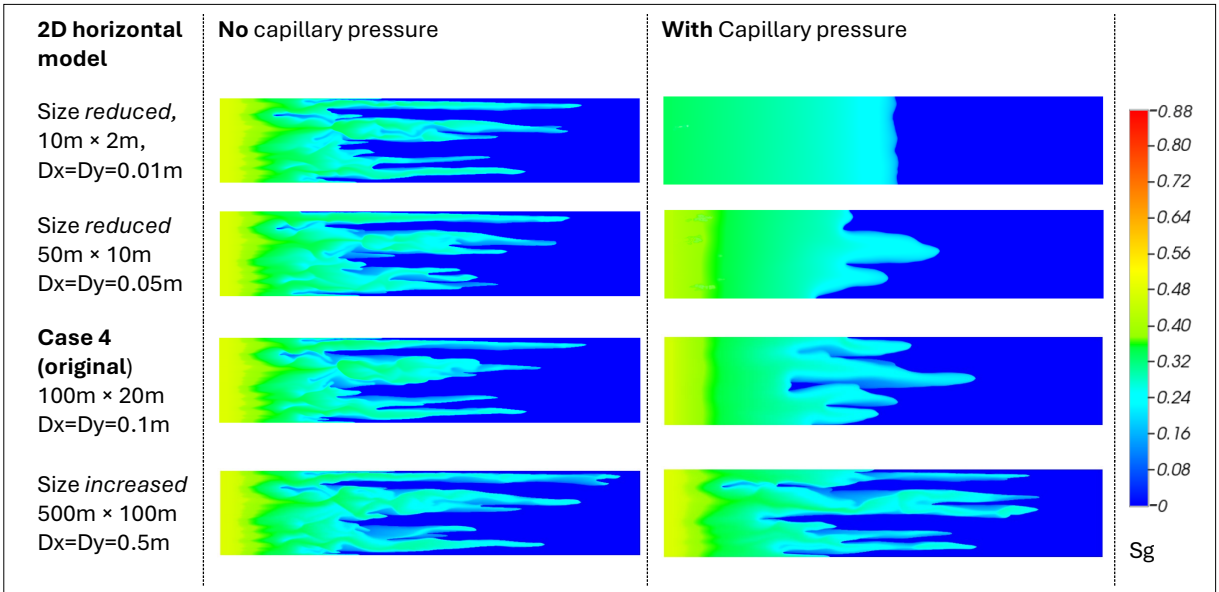


Figure 8: Gas saturation profiles for Case 4 after 0.15 PV of H_2 injection, comparing scenarios varying grid dimensions without (left) and with (32) capillary pressure.

As seen in the left column of **Figure 8**, all four cases without capillary pressure show clear immiscible viscous fingering. The gas displacing front is slightly more advanced in larger models (as indicated by white lines) with the same pore volume injections due to small compressibility effects with H_2. In the right column, the included capillary pressure suppresses the viscous fingers to some extent and retards the gas displacing front (as indicated by right lines). The effect is most marked in the smaller system. In our smallest system tested here (10×2m), the viscous fingering would be totally absent. However, the mitigating impact of capillary dispersivity decreases with the increasing model size and is very minor in the largest model (Bottom row in **Figure 8**; 500m×100m). As model size increases, pressure gradients across the model grow accordingly, leading to more viscous-dominated flow and emergent immiscible fingering.

The question has been raised: *Is there a critical or threshold capillary number where we go from capillary dominated to viscous dominated flow?* This question is addressed in **Appendix B** (available online).

Along with the recommendation raised in the last section, H_2-water relative permeability tests should be conducted in a horizontal orientation at high flow rates to *maximize* the dominance of viscous forces. The rationale is to sustain the viscous fingering patterns and reflect them in the derived RP functions. When a range of RP functions is produced based on the fractional flow curves, the best RP match is selected based on which functions lead to the maximum total mobility λ_T. As noted previously, the total

mobility varying with gas saturations ($\lambda_T(S_g)$ versus S_g) in all of the four cases is plotted in **Figure 6**. The case based on the data by Beteta et al (9) shows a significantly higher total mobility compared to the other three cases. Detailed information on this approach can be found in the literature (9, 10, 29, 32).

4. CONCLUSIONS

The main aim of this work was to point out the inherent errors in relative permeability selection for UHS, and to suggest how these can be remedied. Specifically, three sets of steady-state H_2-water relative permeability datasets widely cited in literature were tested. We identified three key observations.

1. None of the published H_2/water relative permeability datasets properly reflect the unstable flow behavior of H_2 → water in porous media. The main numerical reason for the failure of these published RP curves to show the expected viscous instability is that they lead to total mobilities $\left(\lambda_T(S_g)\right)$ which are *too low*. This then suppresses the fingering. The practical reason such curves arise is that the experiments are not carried out at viscous dominated conditions. In the very small cores, local capillary dispersion dominates, and the core orientation imposes a strong gravity force, which again stabilizes the fingering. Both effects lead to RP curves which yield too low total mobility functions, $\left(\lambda_T(S_w)\right)$, which then predict over-stable displacements.

2. Contrary to the normal practice in conventional methods, core flooding tests for UHS (and other gas/liquid systems) should use larger cores, and the displacement should be performed horizontally and treated as a multi-dimensional flow process. When matching these results by numerical modelling, then viscous fingering (which can be observed) should be assumed in the numerical model. The approach which we have used is to choose the correct fractional flow which matches the two-phase transport correctly and then derive the "maximum mobility RP functions". An example of this was shown through the application of the Case 4 RP curves (9) for simulating H_2 → water displacements.

3. If the fingering RP function described above in Case 4 is used, then it will be limited correctly when either capillary or gravity forces are then introduced into the system. That is, at the small scale, P_c will stabilize the system and stop fingering or when flooded vertically (downwards) at typical flow rates, gravity will suppress the fingering. However, as the system size increases the gas viscous fingering will emerge correctly in the system. In other words, the effects of capillarity are strongly scale-dependent, decreasing as model sizes increase. To accurately assess the interplay of forces involved—including viscous, capillary, and gravitational forces—the application of scaling theory is recommended (10, 35). This approach allows for a more precise evaluation of their relative impacts across different scales, enabling better prediction and control of displacement processes in various reservoir conditions.

STATEMENTS AND DECLARATIONS

Supplementary Material

Appendices to this paper are available online here.

Acknowledgements

We extend our gratitude to the iNetZ+ Global Research Institute at Heriot-Watt University for their support of Dr Gang Wang's research on Underground Hydrogen Storage in his capacity as theme lead. We also acknowledge Energi Simulation for their generous funding of the Chair in CCUS and Reactive Flow Simulation held by Professor Eric Mackay and we thank Professor Arne Skauge for many useful discussions. SLB is also thanked for the use of the Petrel software, and CMG Ltd. for use of the GEM simulator.

Author Contributions

G. Wang: Conceptualization, formal analysis, investigation, methodology, project administration, visualization, writing – original draft, writing – review & editing. **A. Beteta:** Conceptualization, investigation; writing – review & editing. **K. S. Sorbie:** Conceptualization, formal analysis, investigation, methodology, supervision, writing – original draft, writing – review & editing. **E. J. Mackay:** investigation, supervision, writing – review & editing.

Conflicts of Interest

The authors have no conflict of interest to declare.

Data, Code & Protocol Availability

The data that support the findings of this study are available from the corresponding author upon reasonable request.

ORCID IDs

Gang Wang https://orcid.org/0000-0002-2987-177X
Alan Beteta https://orcid.org/0000-0002-3824-0494
Kenneth S. Sorbie https://orcid.org/0000-0002-6841-1529
Eric J. Mackay https://orcid.org/0000-0002-6933-2906

REFERENCES

1. Abdin, Z., Zafaranloo, A., Rafiee, A., Mérida, W., Lipiński, W., & Khalilpour, K. R. (2020). Hydrogen as an energy vector. *Renewable and Sustainable Energy Reviews*, 120, 109620. https://doi.org/10.1016/j.rser.2019.109620
2. Andrews, J., & Shabani, B. (2012). Where does hydrogen fit in a sustainable energy economy? *Procedia Engineering*, 49, 15–25. https://doi.org/10.1016/j.proeng.2012.10.107
3. Aziz, K. and Settari, A. (1979) *Petroleum reservoir simulation*. Applied Science Publishers, London. ISBN 10: 0853347875 ISBN 13: 9780853347873
4. Bade, S. O., Taiwo, K., Ndulue, U. F., Tomomewo, O. S., & Aisosa Oni, B. (2024). A review of underground hydrogen storage systems: Current status, modeling approaches, challenges, and future prospective. *International Journal of Hydrogen Energy*, 80, 449–474. https://doi.org/10.1016/j.ijhydene.2024.07.187
5. Bahrami, M., Izadi Amiri, E., Zivar, D., Ayatollahi, S., & Mahani, H. (2023). Challenges in the simulation of underground hydrogen storage: A review of relative permeability and hysteresis in hydrogen-water system. *Journal of Energy Storage*, 73, 108886. https://doi.org/10.1016/j.est.2023.108886
6. Bennion, B., & Bachu, S. (2005). Relative permeability characteristics for supercritical CO_2 displacing water in a variety of potential sequestration zones in the western Canada sedimentary basin. *SPE Annual Technical Conference and Exhibition*, SPE-95547-MS. https://doi.org/10.2118/95547-MS
7. Berg, S., & Ott, H. (2012). Stability of CO^2–brine immiscible displacement. *International Journal of Greenhouse Gas Control*, 11, 188–203. https://doi.org/10.1016/j.ijggc.2012.07.001
8. Beteta, A., Sorbie, K. S., & McIver, K. (2024). Experimental observations and modeling of the effect of wettability on immiscible viscous fingers at the Darcy scale. *Physics of Fluids*, 36(4), 044111. https://doi.org/10.1063/5.0204036
9. Beteta, A., Sorbie, K. S., McIver, K., Johnson, G., Gasimov, R., & van Zeil, W. (2022). The role of immiscible fingering on the mechanism of secondary and tertiary polymer flooding of viscous oil. *Transport in Porous Media*, 143(2), 343–372. https://doi.org/10.1007/s11242-022-01774-8
10. Beteta, A., Sorbie, K. S., Skauge, A., & Skauge, T. (2024). Immiscible viscous fingering: The effects of wettability/capillarity and scaling. *Transport in Porous Media*, 151(1), 85–118. https://doi.org/10.1007/s11242-023-02034-z
11. Beteta, A., Wang, G., Sorbie, K. S., & Mackay, E. J. (2024). X-ray visualized unstable displacements of water by gas in sandstone slabs for subsurface gas storage. *Physics of Fluids*, 36(10), 102107. https://doi.org/10.1063/5.0224145
12. Bo, Z., Boon, M., Hajibeygi, H., & Hurter, S. (2023). Impact of experimentally measured relative permeability hysteresis on reservoir-scale performance of underground hydrogen storage (UHS). *International Journal of Hydrogen Energy*, 48(36), 13527–13542. https://doi.org/10.1016/j.ijhydene.2022.12.270

13. Boon, M., & Hajibeygi, H. (2022). Experimental characterization of H_2/water multiphase flow in heterogeneous sandstone rock at the core scale relevant for underground hydrogen storage (UHS). *Scientific Reports*, 12(1), 14604. https://doi.org/10.1038/s41598-022-18759-8
14. Chen, X., Gao, S., Kianinejad, A., & DiCarlo, D. A. (2017). Steady-state supercritical CO_2 and brine relative permeability in Berea sandstone at different temperature and pressure conditions. *Water Resources Research*, 53(7), 6312–6321. https://doi.org/10.1002/2017WR020810
15. Honarpour, M., & Mahmood, S. M. (1988). Relative-permeability measurements: An overview. *Journal of Petroleum Technology*, 40(08), 963–966. https://doi.org/10.2118/18565-PA
16. Jerauld, G. R., Davis, H. T., & Scriven, L. E. (1984). Stability fronts of permanent form in immiscible displacement. *SPE Annual Technical Conference and Exhibition*, SPE-13164-MS. https://doi.org/10.2118/13164-MS
17. Jessen, K., Stenby, E. H., & Orr, F. M. (2004). Interplay of phase behavior and numerical dispersion in finite-difference compositional simulation. *SPE Journal*, 9(02), 193–201. https://doi.org/10.2118/88362-PA
18. Johnson, E. F., Bossler, D. P., & Bossler, V. O. N. (1959). Calculation of relative permeability from displacement experiments. *Transactions of the AIME*, 216(01), 370–372. https://doi.org/10.2118/1023-G
19. Kianinejad, A., Chen, X., & DiCarlo, D. A. (2016). Direct measurement of relative permeability in rocks from unsteady-state saturation profiles. *Advances in Water Resources*, 94, 1–10. https://doi.org/10.1016/j.advwatres.2016.04.018
20. Lysyy, M., Føyen, T., Johannesen, E. B., Fernø, M., & Ersland, G. (2022). Hydrogen relative permeability hysteresis in underground storage. *Geophysical Research Letters*, 49(17), e2022GL100364. https://doi.org/10.1029/2022GL100364
21. McPhee, C., Reed, J. and Zubizarreta, I. (2015). Chapter 10: Relative Permeability. In: Mcphee, C., Reed, J. and Zubizarreta, I. (eds.). *Developments in Petroleum Science,* (64). Elsevier, pp. 519-653.
22. Peaceman, D. W. (1977). Fundamentals of numerical reservoir simulation. Elsevier Scientific Pub. Co. Distributors for the U.S. and Canada, Elsevier North-Holland.
23. Peng, D.-Y., & Robinson, D. B. (1976). A new two-constant equation of state. *Industrial & Engineering Chemistry Fundamentals*, 15(1), 59–64. https://doi.org/10.1021/i160057a011
24. Pinder, G. F., Gray, G. G. (2008). *Essentials of Multiphase Flow and Transport in Porous Media*. Wiley. ISBN: 978-0-470-38079-6
25. Rapoport, L. A. (1955). Scaling laws for use in design and operation of water-oil flow models. *Transactions of the AIME*, 204(01), 143–150. https://doi.org/10.2118/415-G
26. Rezaei, A., Hassanpouryouzband, A., Molnar, I., Derikvand, Z., Haszeldine, R. S., & Edlmann, K. (2022). Relative permeability of hydrogen and aqueous brines in sandstones and carbonates at reservoir conditions. *Geophysical Research Letters*, 49(12), e2022GL099433. https://doi.org/10.1029/2022GL099433
27. Riaz, A., & Tchelepi, H. A. (2006). Numerical simulation of immiscible two-phase flow in porous media. *Physics of Fluids*, 18(1), 014104. https://doi.org/10.1063/1.2166388
28. Salmo, I. C., Sorbie, K. S., Skauge, A., & Alzaabi, M. A. (2022). Immiscible viscous fingering: Modelling unstable water–oil displacement experiments in porous media. *Transport in Porous Media*, 145(2), 291–322. https://doi.org/10.1007/s11242-022-01847-8
29. Schlumberger (2022). Petrel technical manual. Schlumberger Limited.
30. Skauge, A., Skauge, T., Sorbie, K. S., Bourgeois, M. J., & Chang, P. L. K. C. (2022). Impact of viscous instabilities on wag displacement. *Paper presented at the ADIPEC, Abu Dhabi, UAE, October 2022*. Paper Number: SPE-211448-MS, D041S127R003. https://doi.org/10.2118/211448-MS
31. Sorbie, K. S., Al Ghafri, A. Y., Skauge, A., & Mackay, E. J. (2020). On the modelling of immiscible viscous fingering in two-phase flow in porous media. *Transport in Porous Media*, 135(2), 331–359. https://doi.org/10.1007/s11242-020-01479-w
32. Taber, J. J., Martin, F. D., & Seright, R. S. (1997). EOR screening criteria revisited— part 1: Introduction to screening criteria and enhanced recovery field projects. *SPE Reservoir Engineering*, 12(03), 189–198. https://doi.org/10.2118/35385-PA
33. Tarkowski, R., & Uliasz-Misiak, B. (2022). Towards underground hydrogen storage: A review of barriers. *Renewable and Sustainable Energy Reviews*, 162, 112451. https://doi.org/10.1016/j.rser.2022.112451
34. Wang, G., Pickup, G. E., Sorbie, K. S., & Mackay, E. J. (2022a). Driving factors for purity of withdrawn hydrogen: A numerical study of underground hydrogen storage with various cushion gases. *SPE EuropEC - Europe Energy Conference Featured at the 83rd EAGE Annual Conference & Exhibition*, D021S001R001. https://doi.org/10.2118/209625-MS

35. Wang, G., Pickup, G., Sorbie, K., & Mackay, E. (2022b). Numerical modelling of H_2 storage with cushion gas of CO_2 in subsurface porous media: Filter effects of CO_2 solubility. *International Journal of Hydrogen Energy*, 47(67), 28956–28968. https://doi.org/10.1016/j.ijhydene.2022.06.201
36. Wang, G., Pickup, G., Sorbie, K., & Mackay, E. (2022c). Scaling analysis of hydrogen flow with carbon dioxide cushion gas in subsurface heterogeneous porous media. *International Journal of Hydrogen Energy*, 47(3), 1752–1764. https://doi.org/10.1016/j.ijhydene.2021.10.224
37. Wu, Y.-S. (2015) *Multiphase fluid flow in porous and fractured reservoirs.* Paperback ISBN: 97801280384829 7 8-0-12-803848–2; eBook ISBN: 9780128039113
38. Yekta, A. E., Manceau, J.-C., Gaboreau, S., Pichavant, M., & Audigane, P. (2018). Determination of hydrogen–water relative permeability and capillary pressure in sandstone: Application to underground hydrogen injection in sedimentary formations. *Transport in Porous Media*, 122(2), 333–356. https://doi.org/10.1007/s11242-018-1004-7
39. Yortsos, Y. C., & Hickernell, F. J. (1989). Linear stability of immiscible displacement in porous media. *SIAM Journal on Applied Mathematics*, 49(3), 730–748. https://doi.org/10.1137/0149043
40. Zivar, D., Kumar, S., & Foroozesh, J. (2021). Underground hydrogen storage: A comprehensive review. *International Journal of Hydrogen Energy*, 46(45), 23436–23462. https://doi.org/10.1016/j.ijhydene.2020.08.138